

Thermal and physical properties of reconsolidated crushed rock salt as a function of porosity and temperature

Stephen Bauer¹ · Alexander Urquhart¹

Received: 1 February 2015 / Accepted: 23 July 2015 / Published online: 8 September 2015
© Springer-Verlag Berlin Heidelberg (outside the USA) 2015

Abstract Crushed salt can be used as backfill to bury and conduct heat away from radioactive waste in salt repositories. As the crushed salt compacts during reconsolidation, its thermal, mechanical and hydrologic properties will change in a manner related to the porosity. Measurements of crushed salt thermal properties are conducted to evaluate such relationships. A simple mixture theory model is presented to predict thermal conductivity of consolidating salt in repository conditions. Experimental work was completed to evaluate the model by measuring thermal conductivity, thermal diffusivity and specific heat of crushed salt as a function of porosity and temperature. Sample porosity ranged from 0 to 46 %, and measurements were made at ambient pressure, from room temperature to 300 °C. These are the temperature conditions expected in a radioactive waste storage facility. Crushed salt thermal conductivity decreases with increasing porosity and temperature. Thermal diffusivity showed little porosity dependence but decreased with increasing temperature. Specific heat also shows little porosity dependence but increases with increasing temperature. Fracture porosity in deformed bedded salt cores appears to reduce thermal conductivity more dramatically than inter- and intra-granular porosity in consolidated salt. A long-term effort to dry crushed salt at high temperatures resulted in a 0.48 weight-percent loss of water that had resided at grain boundaries and in intra-granular fluid inclusions. While this loss does not significantly affect thermal properties, the release of

this water volume could impact the mechanical response of the reconsolidating salt and host rock.

Keywords Backfill · Heat transfer · Nuclear waste isolation · Reconsolidation · Rock mechanics · Thermal properties

1 Introduction

Crushed salt may be used as backfill to isolate and seal heat-generating, medium- to high-level radioactive waste in a salt repository. As the crushed salt conducts heat away from the waste, it will reconsolidate in response to increased temperature, as well as burial pressures. Heat dissipation is an essential function of salt repositories and directly affects the structural evolution of the repository [2, 30]. Predictive modeling of the thermal, mechanical and hydrologic behavior of porous, dynamically reconsolidating crushed salt is therefore critical for repository design. Such modeling requires knowledge of the material properties of crushed salt as it reconsolidates.

This work compares a model of thermal conductivity in porous salt to direct measurements of thermal conductivity and determines the thermal conductivity of reconsolidated crushed salt as a function of porosity and temperature. Thermal diffusivity and specific heat, while not the primary motivation, are also measured. Measurements are made over a range of temperatures expected in repository settings. The mechanisms responsible for observed trends are beyond the scope of this study.

The porosity range of interest in this study is from nearly zero (intact domal and bedded salt, in which repositories may be located) to >40 % (loose salt gravel, which may be used as backfill to isolate radioactive waste). Temperatures

✉ Stephen Bauer
sjbauer@sandia.gov

¹ Geomechanics Department, Sandia National Laboratories, Albuquerque, NM, USA

of interest are from room temperature to 300 °C—a range which likely bounds that in radioactive waste storage facilities. In order to analyze the effects on thermal conductivity of both porosity and temperature, it was necessary to prepare many samples, representing different porosities, and to test each sample at a range of temperatures, resulting in approximately 1700 measurements.

Considerable laboratory work has previously been done to determine the thermal conductivity of both halite and bedded and domal rock salt at a range of temperatures and pressures [1, 9, 10, 13, 20, 22, 25]. The temperature range of interest for these studies is generally from room temperature to as high as 650 °C, with most between room temperature and 300 °C. Confining pressures ranging from ambient to 50 MPa are found to have little effect on thermal conductivity [11, 12, 20]. Some researchers have also acknowledged effects from the composition of the salt, from pure NaCl to salt with up to 20 % insoluble impurities [11, 27, 29]. Additional work has determined thermal conductivity for bedded salt, with no systematic focus on variables within the salt [18]. Birch and Clark [5, 6] developed an early data set for single-crystal halite thermal conductivity.

Although the temperature dependence of rock salt thermal conductivity is well established, little work has been done to determine the effect of porosity. Naturally occurring halite tends to have low porosity, from 0 % for individual crystals to roughly 2–3 % for polycrystalline samples. Limited work has been done on salt samples with higher porosity [1], and this work focused on samples of variable grain and crystal size rather than a systematic analysis of the effects of porosity.

The most comprehensive analysis of the porosity effect is from the combined data of the BAMBUS reports [3, 4], which provide a fairly complete range of salt thermal conductivity values from 0 to 40 % porosity. This study intends to verify and augment these data by systematically measuring porosity effects in a single test series with variable temperature. This will analyze the simultaneous dual controlling effects of porosity and temperature.

1.1 Thermal conductivity model

The geometric mean of rock conductivity and pore conductivity, which estimates bulk thermal conductivity of a two-medium material, can be used to model the thermal conductivity of porous crushed salt [16, citing 24]:

$$\lambda_b = (\lambda_r^{1-n})(\lambda_f^n), \tag{1}$$

where λ is thermal conductivity, b is bulk material, n is porosity, and r and f denote rock and fluid, respectively. Such a model requires accurate temperature-dependent

thermal conductivity values of pure materials. Single-crystal halite values were measured in an extension of this work [28]. Values for air are well known and follow the equation

$$\lambda = (0.0241)(1 + 0.00317T - 0.0000021T^2), \tag{2}$$

where T is temperature in Celsius [17]. Note that the input for (2) is in Celsius, but the equation has been modified from its original form to output units of W/mK rather than the less common Cal./cm C. Inputting values for salt (rock) and air (pore fluid) at different temperatures (Table 1) creates a model of the values likely to be encountered in this work (Fig. 1). We evaluate modeled values against actual measurements.

Visible water loss was noticed during creep tests in which mine-run crushed salt was reconsolidated at high temperatures and pressures. This occurred when the material was first heated and then subjected to confining and shear stresses [8]. Because the presence and introduction of mobile water would have an effect upon salt mechanical response in a repository setting, in addition to measuring thermal conductivity we attempted to dry salt at high temperatures to evaluate the volume fraction of water that could be driven off by heating.

Table 1 Salt thermal conductivity values measured from single-crystal samples [28]

	25 °C	50 °C	100 °C	150 °C	200 °C
λ_{salt}	6.054	5.488	4.658	3.911	3.389
λ_{air}	0.026	0.028	0.031	0.034	0.037

Air thermal conductivity values calculated from Eq. 2 [17]

All values in W/mK

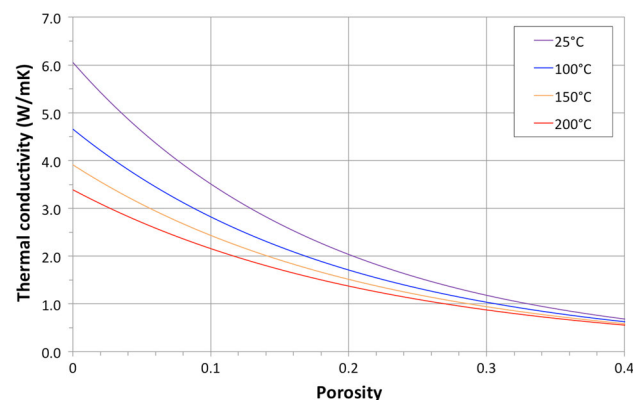


Fig. 1 Estimated thermal conductivity values of crushed salt at a range of repository temperatures

2 Methods

2.1 Sample material and preparation

Samples were composed of compressed crushed salt and cohesive bedded polycrystalline salt from the Waste Isolation Pilot Plant (New Mexico), polycrystalline domal salt from the Port Barre Salt Dome (Louisiana), single-crystal salt from the Hockley Salt Dome (TX) and microcrystalline “solar salt” (salt lick product). The bulk of testing is performed using crushed salt, which can be easily compacted into sample pellets of predetermined porosity and thickness (Fig. 2). This salt is mined from the Waste Isolation Pilot Plant radioactive waste storage facility and therefore represents realistic mineralogy of a storage site, including 1.0–1.6 % water-insoluble impurities. X-ray diffraction analysis of this material shows that it closely resembles previous analyses, which found up to 5 % water-soluble and water-insoluble impurities, including quartz, gypsum and clays [26].

It is difficult to compact salt into samples of 0–2 % porosity. Domal and bedded salt have naturally low porosity, however, and are useful for completing the low-porosity region of the thermal conductivity curve. These salt samples are relatively pure NaCl and do not contain significant amounts of impurities. Minimal porosity is present in the fracture space between crystal boundaries, however.

All crushed salt is sieved to remove grains larger than 9.5 mm in diameter. Variable-porosity samples are formed by compacting crushed salt in a 50-mm die, forming circular pellets roughly 25.4 mm tall. The bulk porosity of these samples is calculated as a ratio of the bulk density of the final pellet to the measured density of crushed salt (2.140 g/cc). Although limited stratification occurs during the pressing process due to grain size sorting, the method used to analyze samples measures bulk thermal conductivity throughout the sample and should average out local sorting. Salt pellets of similar size are formed by coring pellets from bedded and domal salt or solar salt blocks and grinding the ends to a flat surface (Fig. 2).

Two 4-in.-diameter cores of bedded WIPP salt were used to measure the effects of induced fracture porosity on thermal conductivity. The cores have been previously heated—1 to 200 and 1 to 250 °C—and then deformed in uniaxial compression, resulting in “barrel-shaped” deformation and significant fracturing [19]. Each core was cut in half along its vertical axis, and the two faces were polished to enable sandwiching of the thermal properties sensor. Four representative measurement locations were identified on each core face (Fig. 3).

2.2 Thermal conductivity measurements

Measurements were collected over more than 2 years of laboratory effort. Early thermal conductivity data were measured with a Holometrix guarded heat flow meter (TCHM). The TCHM compares the temperature gradient across a sample of known thickness to the flow of heat through the sample in order to calculate sample thermal resistance; thermal resistance is the reciprocal of thermal conductivity (Fig. 4).

The TCHM has a maximum temperature range of 40–200 °C, requires a lengthy calibration and can take up to a day to measure the thermal conductivity of a single sample. A Hot Disk transient plane source thermal constants analyzer (TCA) was therefore acquired to replace the TCHM. The TCA has a greater temperature range (cryogenic to 725 °C), makes measurements more quickly with better than 5 % accuracy and can simultaneously measure thermal conductivity, thermal diffusivity and specific heat. A current passed through the sensor creates a pulse of heat that is absorbed by the sample material. The rate at which the sensor temperature decreases is a function of time and the ability of the sample to conduct heat away from the sensor, which the TCA uses to calculate thermal conductivity, thermal diffusivity and specific heat.

The TCA can measure samples as small as 3 mm in height by 7 mm in diameter, with no maximum size; samples used in this study were mostly disks 50 mm in diameter

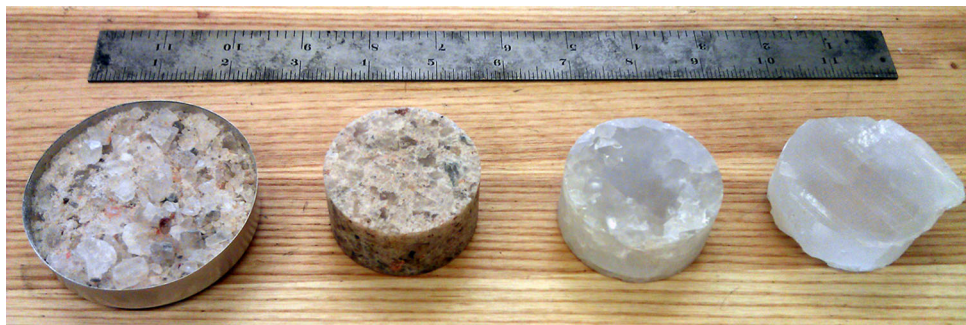


Fig. 2 From *left* loose mine-run crushed salt, die-pressed pellet of mine-run salt, core of relatively pure polycrystalline domal salt, core of single salt crystal. Scale in inches

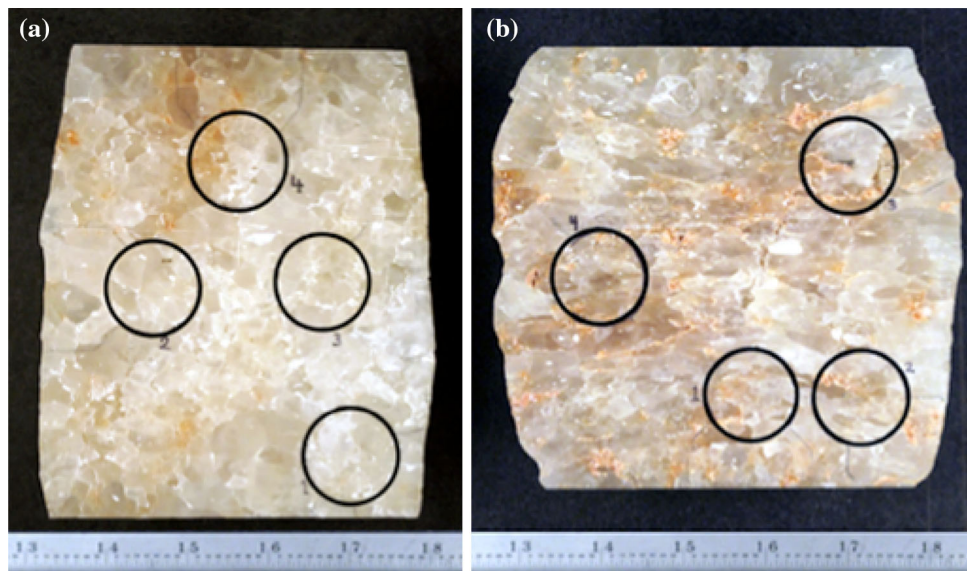


Fig. 3 WIPP core Sample A (a, heated to 200 °C) and Sample B (b, heated to 250 °C), each with four representative measurement locations. Facing halves not shown, scales in inches

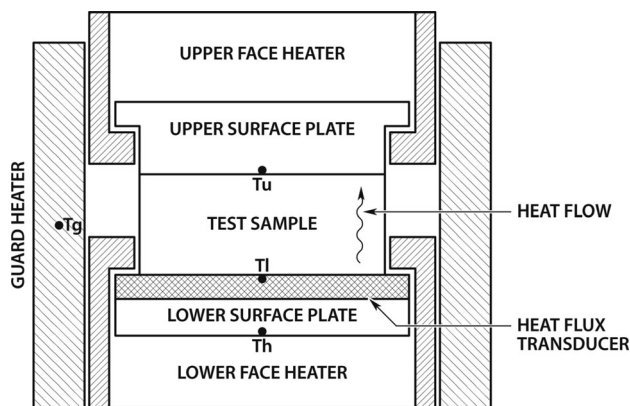


Fig. 4 TCHM assembly: The *upper* and guard heaters maintain a constant temperature difference with the *lower* heater, thermocouples at the *upper* (T_u) and *lower* (T_l) sample surfaces record the temperature gradient across the sample, and the heat flux transducer measures heat flow into the sample

and 25.4 mm tall (Fig. 5). Because the TCA sensor is sandwiched between two halves of a given material, two like-porosity pellets are pressed for each target porosity. The 4-in.-diameter cores (used to evaluate thermal properties of fractured salt) were sliced down their axes, and the sensor was sandwiched between the two halves.

The TCA includes a programmable oven to house the sample and sensor, as well as a computer for data acquisition, data analysis and program control. Measurements were made between room temperature and 200 °C at ambient pressure and moisture conditions. In order to ensure a uniform internal temperature gradient, samples equilibrated at each temperature set point for a few hours before measurements were made. Because data from both

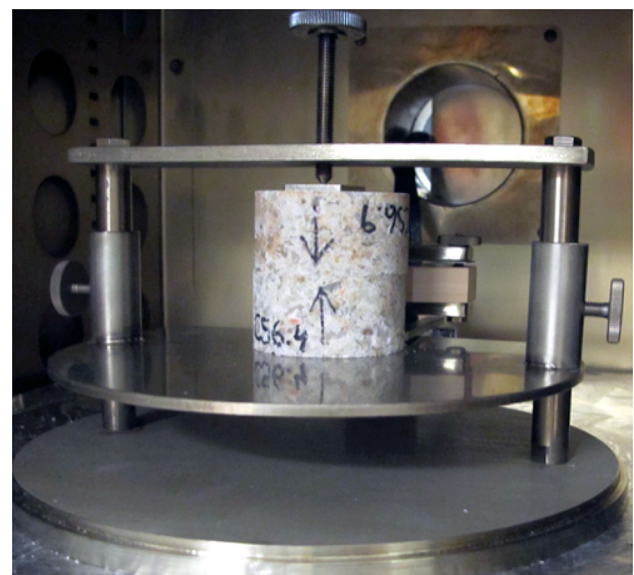


Fig. 5 Two crushed salt pellets sandwiching the planar TCA sensor (inserted from behind). Stack is held together with mounting pressure from the vertical set screw. Assembly is in a computer-controlled oven

the TCA and TCHM are considered equally reliable, all data are reported as a single data set.

2.3 Salt drying

Mine-run crushed salt from the Waste Isolation Pilot Plant was cooked continuously at increasingly high temperatures over a 9-month period in order to estimate the volume of water contained in crushed salt and the amount that could be driven off by heating at ambient pressure. Two uncovered

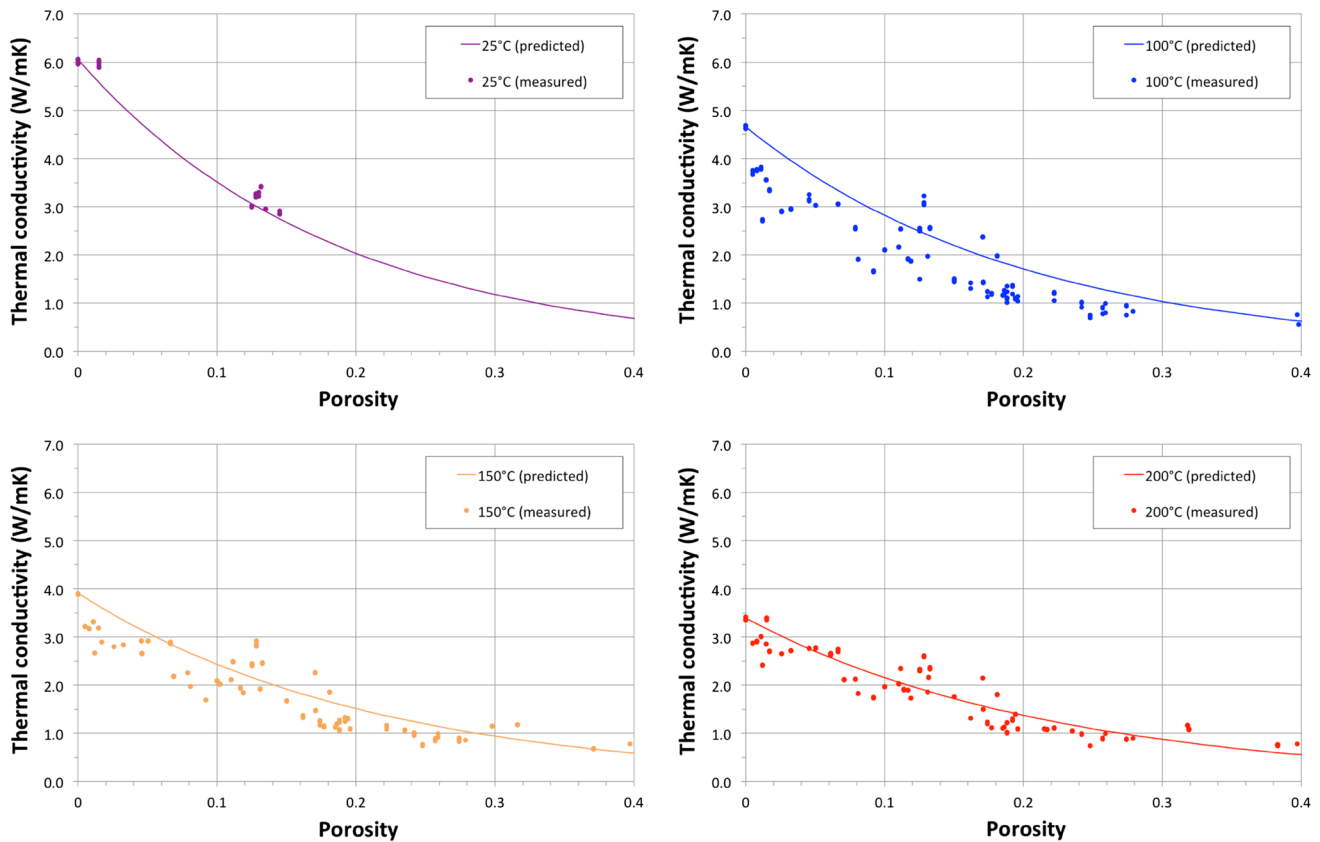


Fig. 6 Measured thermal conductivity (*points*) of variable-porosity salt samples at 25, 100, 150 and 200 °C compared with model-predicted values (*solid lines*) at the same temperatures

tin-plated steel canisters weighing slightly over 300 g each were filled with 2500.0 g each of crushed salt. Grains larger than 9.50 mm in diameter had been previously sieved out. Each canister was weighed at room temperature and then placed in an oven at 50 °C. Oven temperature was raised by 25 °C every 3 weeks, up to 300 °C; temperature was then raised by 50 °C every 3 weeks, up to 400 °C. This process lasted 273 days, with weight measurements taken roughly two out of every 3 days. Samples were always weighed immediately before increasing the temperature as well as the day after the temperature increase. One heating interruption was caused by a power loss some time between April 30 and May 2. Samples were returned to the same temperature and showed a slight drop in weight consistent with the overall data trend at that time.

3 Results

3.1 Thermal conductivity of variable-porosity crushed and polycrystalline salt

Two years of laboratory work produced 1696 thermal conductivity measurements from 80 samples of unique

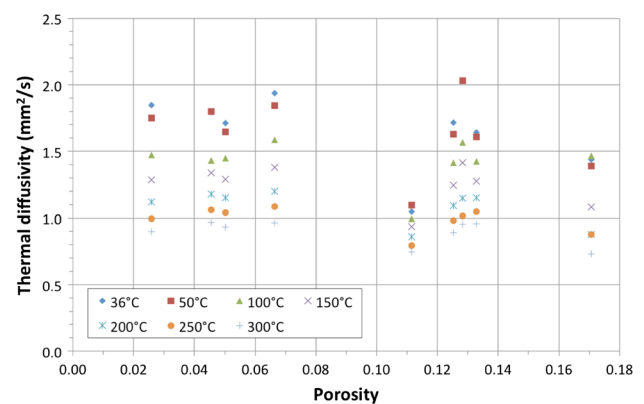


Fig. 7 Thermal diffusivity versus porosity. Thermal diffusivity shows no apparent porosity dependence

porosity; 328 additional measurements of thermal diffusivity and specific heat were taken from ten unique samples. Another 149 measurements of all three thermal properties in single-crystal, optically clear halite are reported in [28]. Samples were analyzed to establish a direct relationship between thermal properties and porosity and temperature. Sample materials ranged in porosity from

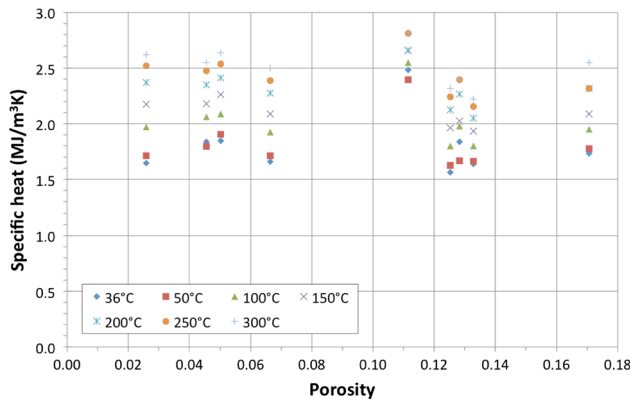


Fig. 8 Specific heat versus porosity. Specific heat shows no apparent porosity dependence

0 % to approximately 46 %—the porosity of unsettled loose salt gravel. Data are segregated by temperature, from 25 to 300 °C.

3.2 Porosity relationship

As shown in Fig. 6, measured thermal conductivities are compared with models of predicted thermal conductivity for any given porosity. Measured thermal conductivity is in most cases slightly lower than model-predicted values, but overall trends follow the model fairly closely. Thermal diffusivity and specific heat results are presented in Figs. 7 and 8, respectively, and show little trend with porosity.

The relationship between thermal properties and temperature is presented in Figs. 9, 10 and 11 (thermal conductivity, thermal diffusivity and specific heat, respectively). These figures show measurements made on single samples as temperature was ramped up to 300 °C. Thermal conductivity of all samples decreases with increasing temperature. This result is consistent with previous research. Thermal diffusivity of all samples also decreases with increasing temperature. Specific heat of all samples increases with increasing temperature. Data from all temperatures and porosities are summarized in Table 2.

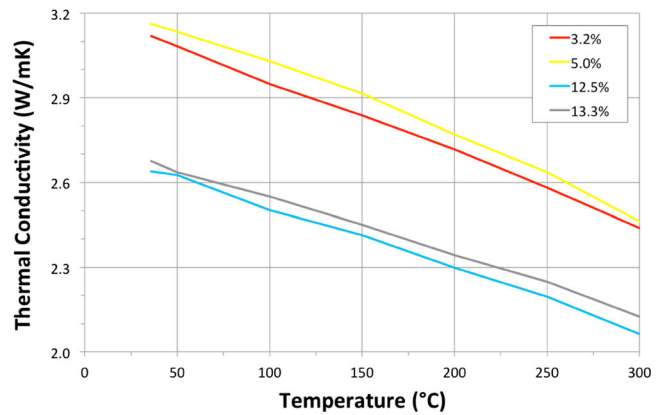
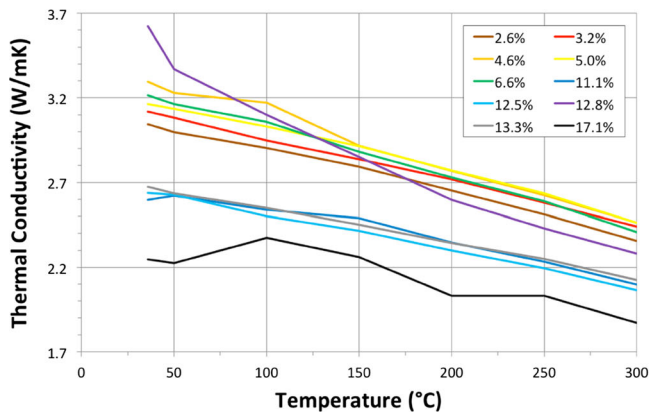


Fig. 9 Thermal conductivity of porous salt samples decreases as the temperature is increased

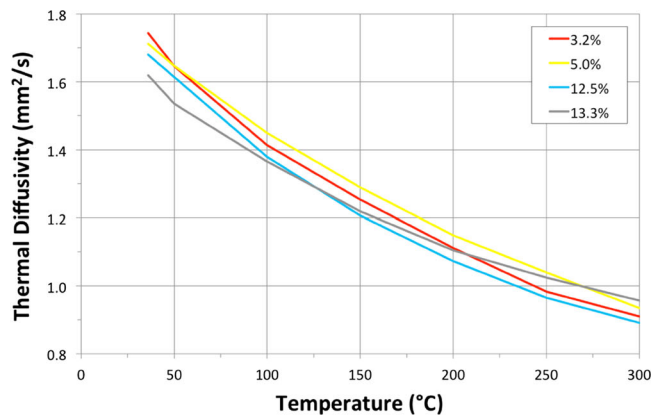
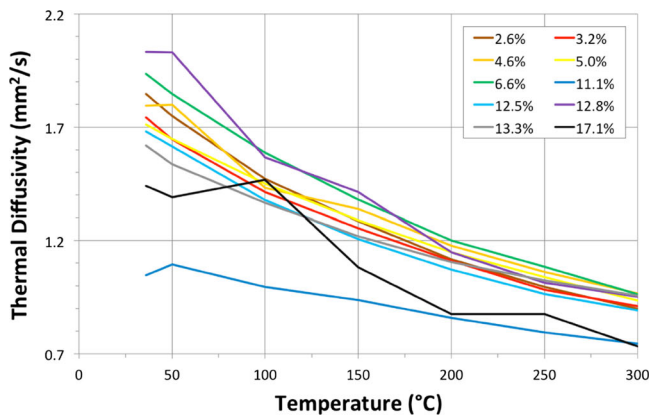


Fig. 10 Thermal diffusivity of porous salt versus temperature samples decreases as the temperature is increased

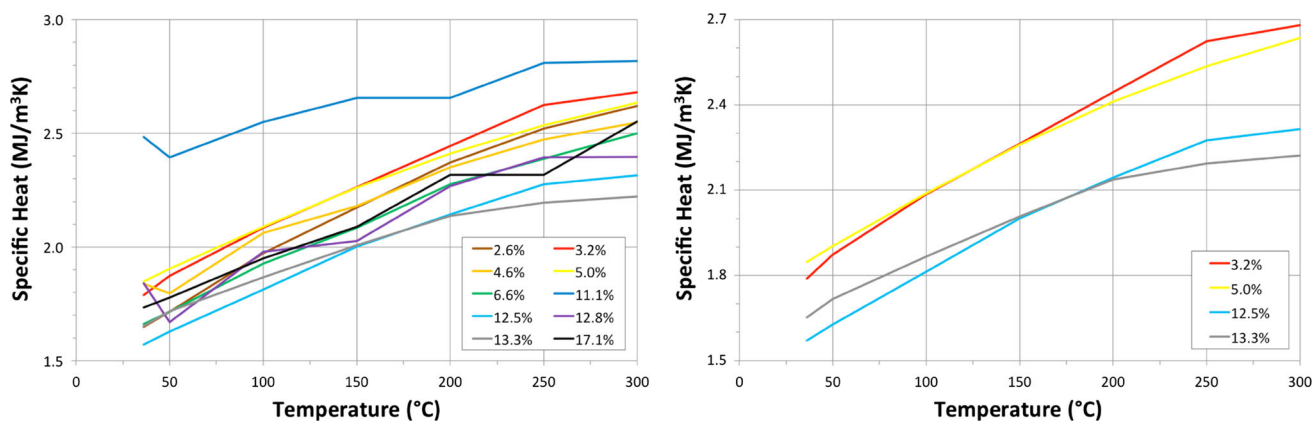


Fig. 11 Specific heat of porous salt samples increases as the temperature is increased

3.3 Thermal conductivity of fractured samples

Thermal conductivity of fractured bedded salt is presented in Figs. 12 and 13. Thermal conductivity ranges from ~ 5.4 to ~ 3.1 W/mK at 25 °C and from ~ 3.0 to ~ 2.0 W/mK at 200 °C. In addition to crack porosity, the deformed salt has <1 % initial porosity. We quantify crack porosity by measuring the linear crack density at the four measurement locations on each sample (Fig. 14). Linear crack density is the number of cracks intersected per unit length in linear traverses across a sample. In addition to grain-cutting linear cracks, most grain boundaries were cracked and some cleavage cracks were observed. Crack aperture was not quantified.

Figures 12 and 13 show thermal conductivity measured at each location on each WIPP core at room temperature, 50, 100, 150 and 200 °C. In Sample A, previously heated to 200 °C, the thermal conductivity at each measurement location drops by an average of 37 % between room temperature and 200 °C; in Sample B, previously heated to 250 °C and showing more deformation than Sample A, the thermal conductivity at each measurement location drops by an average of 41 % between room temperature and 200 °C.

Equation 1 predicts salt thermal conductivity based on porosity. If sample thermal conductivity is known, therefore, porosity can be estimated. In Table 3, the thermal conductivity of the WIPP cores at each location at each temperature is used to estimate porosity at that location.

3.4 Salt drying results

A small volume of brine is present in WIPP salt [15]. This fluid may be adsorbed to grain boundary surfaces, trapped in inter- and intra-crystalline porosity such as negative crystals and fluid inclusions along crystallographic planes or associated with clay mineral impurities. This water can

be liberated by heating the salt. Adsorbed water will evaporate if the salt is heated to 110 °C for a few days, reducing bulk weight by <0.20 % [15]. Fluid inclusions are abundant in both deformed and undeformed bedded salt (Fig. 15); they are sealed in the crystal structure and unable to evaporate at relatively low temperatures. Subjecting the salt to greater heat over a longer period of time shows that more fluid can be released through differential expansion and decrepitation [19]. This was observed in mechanical compression and shear experiments [8], as well as in samples of bedded salt that, when left in an oven at elevated temperature, began to shed small shards of material within the oven.

In an attempt to quantify the trapped volume of water, two canisters of crushed salt were repeatedly weighed while being heated to 400 °C over 9 months (Fig. 16). A total of 175 measurements were made on Canister 1, measuring a change of -11.9 g, for a weight loss of 0.48 %. A total of 174 measurements were made on Canister 2, measuring a change of -12.1 g, also for a weight loss of 0.48 %. Changes in both samples mirrored each other closely throughout the experiment, neither ever exceeding the other in weight loss by more than 0.04 % (Fig. 16). The dramatic drops at 350 and 400 °C are in part due to the greater increase in temperature increments (50 °C as opposed to 25 °C); even so, the loss is greater than at most other consecutive 25 °C intervals and is attributed to polyhalite dehydration, as observed previously in this rock salt [23].

In light of the salt drying data, two sets of samples were heated to 300 °C and then cooled to 50 °C. All three thermal properties were measured during both the heating and cooling legs of this cycle. Values from each leg closely matched each other (Fig. 17), indicating that water loss at high temperatures does not significantly affect thermal properties.

Table 2 Summary of results: modeled and average measured values at key temperatures and porosities

	Average thermal conductivity values at specific porosities and temperatures									
	0.00–4.99 %	5.00–9.99 %	10.00–14.99 %	15.00–19.99 %	20.00–24.99 %	25.00–29.99 %	30.00–34.99 %	35.00–39.99 %	40.00–44.99 %	45.00–49.99 %
36–40 °C	3.08	3.224	2.818	2.075	0.898	0.804	1.005	0.609	0.56	
50 °C	4.264	3.175	2.763	1.484	0.96	0.855	1.005	0.527	0.638	
75 °C	5.085			1.258	0.97	0.874		0.659	0.633	
100 °C	3.618	2.687	2.385	1.477	0.934	0.89	1.173	0.63	0.726	
125 °C	3.769	2.177	1.988	1.337	1.087	0.863			0.666	
150 °C	2.961	2.548	2.323	1.499	0.957	0.913	1.163		0.638	
175 °C	3.225	2.139	1.983	1.162	0.957	0.913	1.163		0.638	
200 °C	3.152	2.426	2.135	1.636	1.038	0.99	1.087		0.639	
225 °C	3.199									
250 °C	2.823	2.616	2.26	2.03						
275 °C	2.864									
300 °C	2.548	2.444	2.142	1.87						

Values in bold are the mean of fewer than 10 data points
All values in W/mK

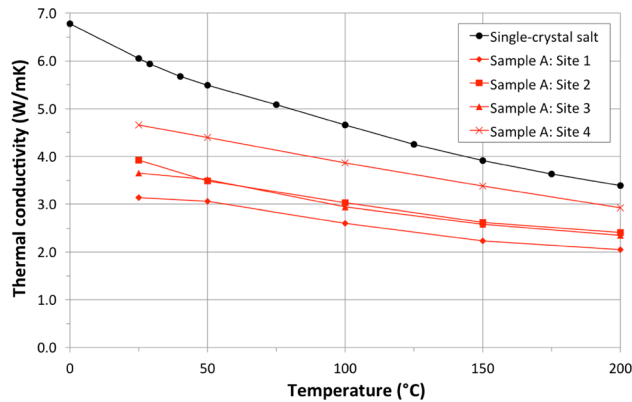


Fig. 12 Sample A thermal conductivity data compared to single-crystal (0 % porosity) salt thermal conductivity data

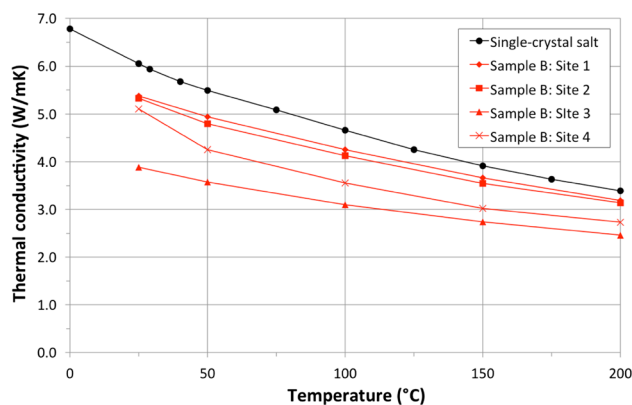


Fig. 13 Sample B thermal conductivity data compared to single-crystal (0 % porosity) salt thermal conductivity data

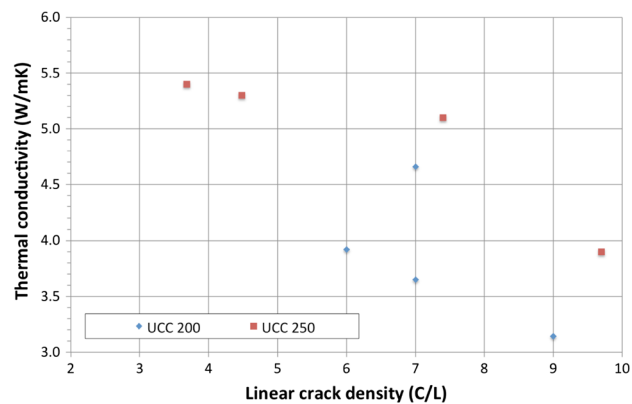


Fig. 14 Linear crack density versus thermal conductivity

4 Discussion

4.1 Porosity and temperature effects on thermal conductivity

The primary focus of this work is to measure the thermal properties of reconsolidating crushed salt, in order to

Table 3 Estimated porosity of WIPP core measurement sites based on comparison with single-crystal thermal conductivity

Site	WIPP core TC as fraction of single-crystal TC						Estimated porosity (%)
	25° (%)	50° (%)	100° (%)	150° (%)	200° (%)	Avg. (%)	
A1	52	56	56	57	61	56	~12
A2	65	64	65	67	71	66	~8
A3	60	64	63	66	70	65	~10
A4	77	80	83	87	87	83	~4
B1	89	90	91	94	94	92	~2
B2	88	87	89	91	93	90	~2
B3	64	65	66	70	73	68	~8
B4	84	78	76	77	81	79	~5

TC thermal conductivity

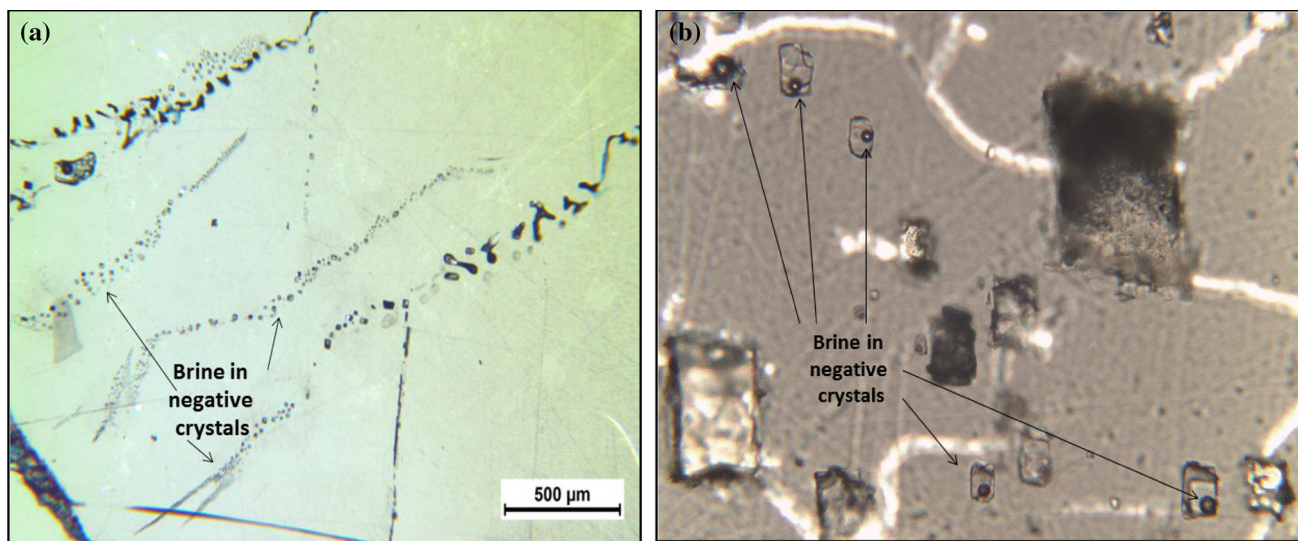


Fig. 15 **a** Inter-granular fluid inclusions lining up along crystallographic planes, **b** intra-granular negative crystals with brine fluid inclusions and gas bubble, fields of view 200 μm across

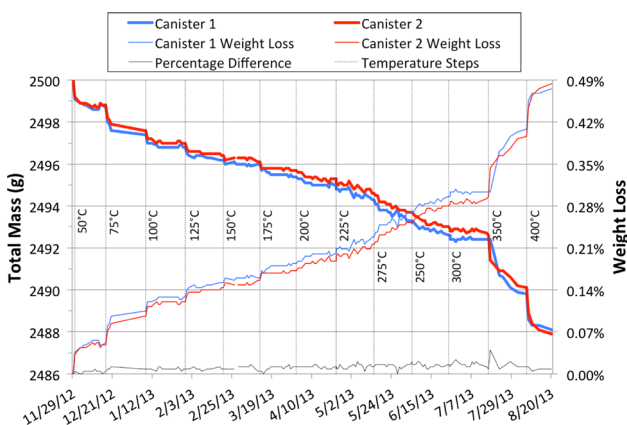


Fig. 16 Salt drying history from two canisters. Note that the total percentage weight loss of each sample is nearly the same at all times; the difference in percentage lost is never greater than 0.04 %

identify the effects of porosity and temperature, especially on thermal conductivity. Nearly 1700 thermal properties’ measurements were made over a range of salt porosities and temperatures.

Using single-crystal halite thermal conductivity data and published air thermal conductivity data, a model was created to estimate the thermal conductivity of porous crushed salt backfill which may be used to analyze radioactive waste repositories response. Measurements of crushed salt thermal conductivity are close to those predicted by the model throughout the repository-like range of porosities and temperatures. This supports use of Eq. 1 as a good predictor of porous salt thermal conductivity over a range of likely radioactive waste storage conditions.

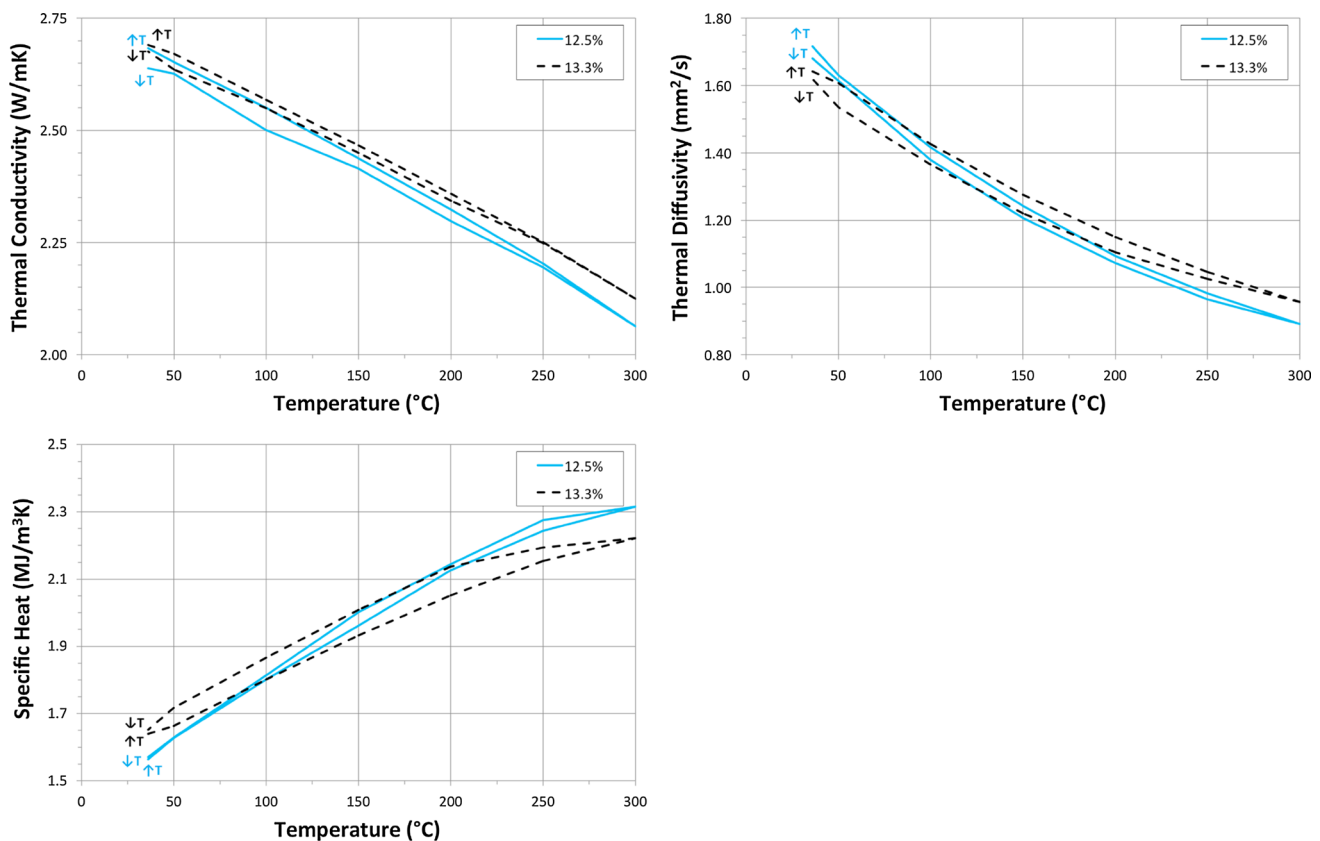


Fig. 17 Thermal conductivity, thermal diffusivity and specific heat show no systematic change in samples heated to 300 °C and returned to 50 °C, despite the estimated loss of up to 0.48 % water mass

Thermal conductivity was found to decrease with increasing porosity and increasing temperature. The magnitude of the temperature effect is greatest at low porosities; at high porosities, there is virtually no noticeable temperature effect. This can be explained by the conductivity of air, which is two orders of magnitude lower than that of salt. At higher porosities, the conductivity of air becomes increasingly overwhelming. Although air conductivity also goes down with increasing temperature, the difference is relatively small compared to the bulk thermal conductivity of porous rock salt.

Thermal diffusivity shows little correlation with porosity, but decreases with increasing temperature. Specific heat also shows little porosity dependence, but increases with increasing temperature. Among the measurements collected, thermal conductivity is the only property that exhibits a temperature dependence. Together, these results can be used to model salt-backfilled radioactive waste storage sites. Thermal conductivity of the backfill will increase as the crushed salt compacts under pressure. This will result in increasingly efficient dissipation of heat as time progresses. The effect of heating from radioactive waste will in part counter this increase in thermal conductivity, however, as crushed salt

at any porosity will have a lower thermal conductivity when heated.

4.2 Fractured samples

It is reasonable to expect crack porosity to affect thermal properties differently than inter- and intra-granular porosity. Thermal conductivity measurements were made from 25 to 200 °C and at ambient pressure on deformed bedded rock salt with varying amounts of impurities and crack porosity. Thermal conductivity for deformed bedded rock salt, which contains small amounts of impurities and pore porosity, is lower than that of single-crystal salt by 10–50 %, independent of temperature. This is hypothesized to be caused by the presence of open fractures between and through salt crystals. Fractures increase porosity, which is shown to reduce thermal conductivity. The effect of the presence of fractures appears to diminish with increasing temperature. This is perhaps because thermal expansion causes the cracks to close a small amount at higher temperatures, reducing fracture porosity and increasing conductance by contact.

Porosity estimates of the deformed salt can be made by comparing measured thermal conductivity to the thermal

conductivity model derived from Eq. 1. The 50 % decrease in thermal conductivity observed in fractured salt corresponds to a predicted 12–15 % increase in porosity. That level of porosity is not observed in the deformed samples when analyzed under an optical microscope. This implies that crack porosity imposes discontinuities upon conductivity and may affect conductivity in a different manner than pore porosity.

The lowest thermal conductivities correspond roughly to the greatest linear crack densities, indicating that deformation-induced fracture porosity is the predominant control on thermal conductivity. At some locations, however, other features appear to overwhelm the influence of crack porosity on thermal conductivity. These features, including impurities and additional pore porosity that vary from sampling point to sampling point, degrade the definitive relationship between crack density and thermal conductivity.

4.3 Salt drying

Rock salt contains abundant fluid inclusions that lock water into a crystal reservoir. The volume of water expelled during heating and subsequent mechanical testing is likely drawn from these fluid inclusions as the salt is heated and fluid pressures exceed local crystal strength; also, crystals sheared under pressure facilitate migration of fluids to grain boundaries allowing the fluids a means of escape [8]. Optical microscopy on salt crystals before and after deformation shows that many fluid inclusions have been released. This is a likely explanation for the fluid release observed during mechanical compaction and shear testing. Even in the absence of pressure and shear strain, however, heating crushed salt to 400 °C still releases significant trapped water. The most likely mechanism of release is differential thermal expansion. As fluid inclusions are heated, pressure within a negative crystal builds and eventually exceeds crystal strength leading to fracture, reducing pressure and releasing trapped water via flow through the fracture.

In a 2500-g sample, a 0.48 % weight loss equates to about 12 g, or 12 cc of water. Assuming a crushed salt density of 2.14 g/cc [7, 14, 21], this water volume represents about 1.0 % of the bulk crushed salt volume. Weight loss is closely mirrored in both canisters, indicating that these data are representative of greater trends and may be relatively insensitive to heterogeneities in source material.

It is apparent that water can be released at all temperatures of repository interest, from room temperature to above 300 °C. The existence and potential release of this brine have implications for radioactive waste repository modeling. Although no thermal properties appear significantly impacted by the loss of trapped water, the

assumption of a dry environment is invalid if 1 % of backfill volume is potentially a water reservoir. If sufficient water is liberated by heating and burial pressure, engineered solutions may be necessary to prevent corrosion of waste containers and to transport the water out of the repository. It is perhaps equally important to understand the impact of such water volume upon mechanical response.

5 Conclusions

During the course of this study, close to two thousand thermal conductivity measurements were made over a range of porosities and temperatures. Thermal conductivity of porous salt was found to decrease with increasing porosity and decrease with increasing temperature. Thermal diffusivity and specific heat showed less porosity dependence. All thermal properties showed strong temperature dependence, however: Thermal conductivity and specific heat decrease with increasing temperature, while specific heat decreases with increasing temperature. Additional measurements on uniaxially deformed bedded salt cores showed that an equal amount of fracture porosity may have a larger effect on thermal conductivity than pore porosity.

Subjecting crushed salt to temperatures as high as 400 °C releases a volume of water previously trapped in fluid inclusions. Because it is trapped within the crystal, this brine is not driven off at standard drying temperatures of 110 °C, but higher temperatures cause it to crack the crystal and escape. The volume released appears too small to significantly affect the thermal properties of the crushed salt. The cumulative effect in a repository setting should perhaps be included in performance assessments, however, as engineered solutions may be required to divert water away from waste containers.

Acknowledgments This work was completed in the Geomechanics Laboratory at Sandia National Laboratories. Sandia National Laboratories is a multiprogram laboratory managed and operated by Sandia Corporation, a wholly owned subsidiary of Lockheed Martin Corporation, for the U.S. Department of Energy's National Nuclear Security Administration under contract DE-AC04-94AL85000.

References

1. Acton U (1977) Thermal conductivity of SE New Mexico rock-salt and anhydrite. In: Proceedings of the international conference on thermal conductivity, 15th, Ottawa, 1977, SAND-77-0962
2. Aubertin M, Hardy HR (1996) The mechanical behavior of salt. In: Proceedings of the fourth conference. Montreal Canada. Trans Tech Publications. ISBN 0-87849-103-1
3. Bechthold W, Rothfuchs T, Poley A, Ghoreychi M, Heusermann S, Gens A, Olivella S (1999) Backfilling and sealing of underground repositories for radioactive waste in salt (Bambus

- Project): Final Report. EUR 19124 EN. European Commission, Brussels
4. Bechthold W, Smailos E, Heusermann S, Bollingerfehr W, Bazargan Sabet B, Rothfuchs T, Kamlot P, Grupa J, Olivella S, Hansen F (2004) Backfilling and sealing of underground repositories for radioactive waste in salt (Bambus II Project): Final Report. EUR 20621 EN. European Commission, Luxembourg
 5. Birch F, Clark H (1940) The thermal conductivity of rocks and its dependence upon temperature and composition: part 1. *Am J Sci* 238:529–558
 6. Birch F, Clark H (1940) The thermal conductivity of rocks and its dependence upon temperature and composition: part 2. *Am J Sci* 238:613–635
 7. Brodsky N, Zeuch D, Holcomb D (1995) Consolidation and permeability of crushed WIPP salt in hydrostatic and triaxial compression. In: Proceedings of the 35th U.S. symposium on rock mechanics, pp 497–502
 8. Broome ST, Bauer SJ, and Hansen FD (2014) Reconsolidation of crushed salt to 250 °C under hydrostatic and shear stress conditions. In: 48th US rock mechanics/geomechanics symposium
 9. Durham WB, Abey AE (1981) Effects of pressure and temperature on the thermal properties of a salt and a quartz monzonite. UCRL-85285. Lawrence Livermore National Laboratory, Livermore, CA
 10. Durham WB, Abey AE, Trimmer DA (1981) Thermal properties of Avery Island rock salt to 573 K and 50 MPa confining pressure. UCRL-53128. Lawrence Livermore National Laboratory, Livermore, CA
 11. Durham WB, Abey AE, Trimmer DA (1983) Thermal conductivity, diffusivity and expansion of Avery Island salt at pressure and temperature. In: Larsen DC (ed) Thermal conductivity 16. Plenum Publishing Corp., New York
 12. Durham WB, Boro CO, Beiriger JM, Montan DN (1983) Thermal conductivity of Permian Basin bedded salt at elevated pressure and temperature. UCRL-53476. Lawrence Livermore National Laboratory, Livermore, CA
 13. Durham WB, Boro CO, Beiriger JM (1984) Thermal conductivity of Permian Basin bedded salt at elevated pressure UCRL-90725, CONF-8310163-11. Lawrence Livermore National Laboratory, Livermore, CA
 14. Hansen F, Callahan G, van Sambeek L (1993) Reconsolidation of salt as applied to permanent seals for the Waste Isolation Pilot Plant. In: Proceedings of the 3rd conference on the mechanical behavior of salt, Transtech Publications, Palaiseau, France, pp 323–335
 15. Hansen F, Ahrens E, Tidwell V, Tillerson J, Brodsky N (1995) Dynamic compaction of salt: initial demonstration and performance testing. In: Daemen J, Schultz R (eds) Proceedings of the 35th U.S. symposium on rock mechanics, Brookfield, VT, pp 755–760
 16. Ingebritsen S, Sanford W, Neuzil C (2006) Groundwater in geologic processes, 2nd edn. Cambridge University Press, Cambridge
 17. Kannuluik WG, Carman EH (1951) The temperature dependence of the thermal conductivity of air. *Aust J Sci Res Ser A Phys Sci* 4:305
 18. Liu S, Feng C, Wang L, Cheng L (2011) Measurement and analysis of thermal conductivity of rocks in the Tarim Basin, Northwest China. *Acta Geol Sin* 85:598–609
 19. Mellegard K, Callahan G, Hansen F (2013) High-temperature characterization of bedded Permian salt. In: 47th US rock mechanics/geomechanics symposium
 20. Morgan MT (1979) Thermal conductivity of rock salt from Louisiana salt domes ORNL/TM-6809. Oak Ridge National Laboratory, Oak Ridge, TN
 21. Brodsky N (1994) Hydrostatic and shear consolidation tests with permeability measurements on Waste Isolation Pilot Plant crushed salt, SAND93-7058. Sandia National Laboratories, Albuquerque, NM
 22. Robertson E (1988) Thermal properties of rocks. Report 88-441. US Geological Survey, Reston, VA
 23. Roedder E, Bassett RL (1981) Problems in determination of the water content of rock-salt samples and its significance in nuclear-waste storage siting. *Geology* 9:525–530
 24. Sass JH, Lachenbruch AH, Munroe RJ (1971) Thermal conductivity of rocks from measurements on fragments and its application to heat-flow determinations. *J Geophys Res* 76:3391–3401
 25. Smith DD (1976) Thermal conductivity of halite using a pulsed laser, Oak Ridge Y-12 Plant. Y/DA-7013
 26. Stein C (1985) Mineralogy in the Waste Isolation Pilot Plant (WIPP) facility stratigraphic horizon SAND85–0321. Sandia National Laboratories, Albuquerque, NM
 27. Sweet JN, McCreight JE (1979) Thermal conductivity of rocksalt and other geologic materials from the site of the proposed waste isolation pilot plant. SAND79-1134, SAND79-1134. Sandia National Laboratories, Albuquerque, NM
 28. Urquhart A, Bauer S (2015) Experimental determination of single-crystal halite thermal conductivity, diffusivity and specific heat from –75 °C to 300°C. *Int J Rock Mech Min Sci*. doi:10.1016/j.ijrmms.2015.04.007
 29. van den Broek WMGT (1982) Impurities in rock-salt: consequences for the temperature increases at the disposal of high-level nuclear waste. PB-83-102087. Technische Hogeschool Delft, Netherlands
 30. Wallner M, Lux K-H, Minkley W, Hardy HR (2007) The mechanical behavior of salt. In: Proceeding of the sixth conference, Hannover, Germany. Balkema. ISBN 13: 978-415-444398-2